Structural Features of Parathyroid Hormone Receptor Coupled to $G\alpha_S$-Protein

Jessica Plati,* Natia Tsomaia,† Andrea Piserchio,† and Dale F. Mierke*†
*Department of Chemistry, and †Department of Molecular Pharmacology, Division of Biology & Medicine, Brown University, Providence, Rhode Island

ABSTRACT The molecular basis of the activation of G-proteins by the G-protein coupled receptor for parathyroid hormone (PTH) is unknown. Employing a combination of NMR methods and computer-based structural refinement, structural features involved in the activation of $G\alpha_s$ by the PTH receptor (PTH1R) have been determined. Focusing on the C-terminus of the third intracellular loop (IC3), previously shown to be important for $G\alpha_s$ activation by PTH1R, the structure of this region, PTH1R(402–408), while bound to $G\alpha_s$, was determined by transferred nuclear Overhauser effect spectroscopy. The relative topological orientation of the IC3 while associated with $G\alpha_s$ was determined by saturation transfer difference spectroscopy. These experimental data were incorporated into molecular dynamics simulations of the PTH1R and $G\alpha_s$ to provide atomic insight into the receptor-protein interactions important for PTH signaling and a structural framework to analyze previous mutagenesis studies of $G\alpha_s$. These data provide the first step toward development of a molecular mechanism for the signaling profile of PTH1R, an important regulator of calcium levels in the bloodstream.

INTRODUCTION

Parathyroid hormone (PTH) is a major regulator of blood calcium levels and bone homeostasis (1,2). The hormone acts by way of the PTH/PTHrP receptor (PTH1R), a G-coupled-protein receptor (GPCR), associated with both cyclic adenosine-monophosphate (cAMP) and inositol triphosphate/intracellular calcium signaling pathways (2–5), associated with the activation of $G\alpha_s$ and $G\alpha_q$, respectively. The basis of the specificity of PTH1R for G-proteins, which structurally are similar (6–8), is not fully understood.

The C-terminus of the α-subunits of G-proteins ($G\alpha$) has been established as crucial in the interaction between $G\alpha_s$ and GPCRs. Receptor-mediated accumulation of cAMP is blocked by peptide-specific antibodies that bind to the 10 most distal carboxy terminal residues (9,10). In addition, experimentally and genetically generated mutations located in this region of $G\alpha_s$ uncouple the G-protein from the receptor (11). Specifically, the C-terminal mutation R385H (12) and R389P (13,14) lead to uncoupling of $G\alpha_s$ from all GPCRs, and the deletion of Ile-382 specifically uncouples $G\alpha_s$ from PTH1R (16). (For clarity in the description of the interaction between the receptor and G-protein, residues are denoted by the three-letter code and single-letter code for PTH1R and G-protein, respectively.) The deletion of Ile-382 possibly causes a destabilization of the contact between the α5 helix and the α4-β6 loop of $G\alpha_s$ by altering the kink located in the middle of the α5 helix (16). The specific uncoupling of $G\alpha_s$ indicates the importance of the relative orientations of these secondary structural domains in the interaction between $G\alpha_s$ and PTH1R.

Although the significance of the C-terminus of G-proteins in contacting GPCRs has been demonstrated in previous studies, receptor specificity is not dictated by the C-terminus alone. In chimeric studies, the ability of a $G\alpha$ carboxy terminus to confer receptor specificity on the $G\alpha$ chimera depends on the receptor with which it is paired (17,18). For example, replacing the five C-terminal amino acid residues of $G\alpha_q$ with those of $G\alpha_s$ produced a $G\alpha_q$ chimera that was able to stimulate phospholipase C in the α_s-coupled V2 vasopressin receptor but not the α_s-coupled β_2-adrenergic receptor (17). Also, chimeric $G\alpha_s$ protein with the five C-terminal residues replaced with those of $G\alpha_q$ was able to stimulate adenylate cyclase in the α_q-coupled bombesin and V1a vasopressin receptors but not the α_q-coupled oxytocin receptor (17). Therefore, additional, unidentified residues of $G\alpha_s$ are likely to contact the receptor (19). Evolutionary trace analysis, a method that uses evolutionary conserved residues to predict binding surfaces of proteins that are similar in structure but differ in function, indicates that the receptor binding site of $G\alpha_s$ (20) involves the sixth β-strand β6, the N-terminal ends of β4 and β5, and the C-terminus. Studies in which mutations of the solvent exposed residues R280, T284 and I285 in the α3-β5 loop of $G\alpha_s$ decreased the β_2-adrenergic receptor-mediated accumulation of cAMP without affecting guanine nucleotide binding or hydrolysis (19) support the possibility of the N-terminal end of β5 contacting the receptor.

The significance of the N- and C-terminal 8–15 residues of the third intracellular loop (IC3) of GPCRs in coupling to G-protein has been established (21). For PTH1R, the deletion of the 5 C-terminal amino acids produced a 97%

Submitted August 4, 2006, and accepted for publication September 12, 2006.

Address reprint requests to Dale F. Mierke, Dept. of Molecular Pharmacology, Div. of Biology & Medicine, Box G-B4, Brown University, Providence, RI 02912. Tel.: 401-863-2139; Fax: 401-863-1595; E-mail: dale_mierke@brown.edu.

Andrea Piserchio's present address is New York Structural Biology Center, 89 Convent Ave., New York, New York, 10027.

0006-3495/07/01/535/06 $2.00

doi: 10.1529/biophysj.106.094813

reduction in cAMP, but retained 50% of its ability to increase IPs (22), indicating the importance of the C-terminus of IC3 in $G\alpha_s$. To provide molecular insight into this interaction, we have undertaken the structural characterization of PTH1R(402–408), containing the important residues previously identified while coupled to $G\alpha_s$. Previously we have determined the structure of the IC3 of PTH1R whereas free both in aqueous solution and associated with a membrane environment (23,24), demonstrating structural features at both the N- and C-termini of the IC3. These results clearly illustrate the hydrophobic residues of PTH1R(402–408) are in close contact to $G\alpha_s$, and in particular to those residues previously implicated in $G\alpha_s$ activation.

METHODS

Construction of $G\alpha_s$ expression vector

The cDNA of $G\alpha_s$ long was obtained from the UMR cDNA resource center. Standard PCR methods were used to clone the coding sequence of $G\alpha_s$ with a 5′ *Nco*1 restriction site and a 3′ *Xho*1 restriction site. The PCR product was digested and ligated into the pCal-n-EK vector (Stratagene, La Jolla, CA). Sequencing of the plasmid using the T7 promoter primer was performed by Agencourt (Beverly, MA).

Expression and purification of $G\alpha_s$

Escherichia coli strain BL21 Star™ (DE3), transformed with the sequenced plasmid, was used to inoculate 50 mL of LB Broth. The culture was grown overnight at 37°C and was then used to inoculate 2.5 L of LB broth. At $OD_{600} = .60$, the culture was induced with 2.5 mL of 1M IPTG. The culture was grown for 16 h at 18°C. *E. coli* was harvested by centrifugation at 6,000 rpm for 30 min at 4°C. Cell pellets were resuspended in 50 mM Tris-HCl (pH = 8.0), 150 mM NaCl, 2 mM DTT, 1.0 mM magnesium acetate, 1.0 mM imidazole, 2 mM $CaCl_2$. French pressure cell press was used to lyse the cells at 11,000 psi. The lysate was centrifuged at 12,000 rpm for 30 min at 4°C. The supernatant was incubated with 2 mL bed volume of calmodulin affinity resin (Stratagene) on a rotisserie for 5 h at 4°C. The beads were washed with lysis buffer and high salt lysis buffer (300 mM NaCl). The elution buffer (50 mM Tris-HCl (pH = 8.0), 2 mM DTT, 2 mM EGTA, 1 M NaCl) was used to elute $G\alpha_s$ from the column in eight 1.5 mL fractions. A sample of each fraction was run on a 10% NuPAGE™ Bis-Tris gel (Invitrogen, Carlsbad, CA) with MOPS running buffer (Invitrogen). The fractions were combined and concentrated to 500 μL using Vivaspin4 concentrator (Vivascience) with a 5000 MWCO, PES membrane. The protein was dialyzed into 20 mM Na_2HPO_4, 2 mM DTT, pH = 7 using a 500 μL Float-a-lyzer with a 500 MWCO, cellulose ester membrane (Spectrum, Edgewood, NY).

Nuclear magnetic resonance

Transferred NOEs experiments (25–27) were performed on a mixture of 70 μM $G\alpha_s$ and 1 mM PTH1R(402–408), a peptide composed of the seven C-terminal residues, Glu-Tyr-Arg-Lys-Leu-Leu-Lys, of IC3 of PTH1R in 20 mM phosphate buffer, pH 7.0, containing 2 mM deuterated DTT and TSP as an internal chemical shift reference. The NMR experiments were performed on a Bruker Avance spectrometer with proton resonance frequency of 600.1 MHz. The peptide is in fast exchange, between the bound and the free state producing large, negative NOEs, indicating association with $G\alpha_s$. NMR experiments followed previously published procedures (28). The peaks of the acquired trNOESY experiments, with different mixing times from 50 to 300 ms, were assigned and integrated. Distance geometry calculations, which used constraints generated from holonomic distance bounds and the distances generated by the NOEs, were performed to determine initial structures used for further refinement following methods previously described (28). Saturation-transfer-difference (STD) NMR experiments were carried out with similar sample conditions as the trNOEs, by selective saturation of the $G\alpha_s$ and subtraction of spectra without saturation. In the one-dimensional STD experiment the on-resonance selective irradiation of the Gsα protein (employing a 50-ms long Gauss-shaped pulse separated by a 1-ms delay) was applied at −0.3 ppm. For the reference spectrum, off-resonance irradiation was applied at 30 ppm. Subtraction of the one-dimensional STD spectra was performed internally via phase cycling after every scan. The spectral width for all one-dimensional STD experiments was 16 ppm. All spectra were recorded with T1ρ filter to eliminate the background protein resonances. The total number of scans was 48 with relaxation delay of 5 s. The water suppression was achieved with WATERGATE scheme.

Molecular modeling

The model of the PTH1R(402–408) peptide bound to $G\alpha_s$ protein, was constructed using the bound peptide conformation, as determined by TRNOEs, and the crystal structure of $G\alpha_s$ (33). The relative orientation of the peptide with respect to G-protein was defined by STD NMR data. In addition, previous mutational studies, alanine scanning, and evolutionally trace analyses have provided a good description of a tentative binding pocket on $G\alpha_s$.

This pocket was sampled with 20 starting conformations of PTH1R(402–408)/$G\alpha_s$, and most energetically stable has been chosen for extensive MD simulations, performed with the GROMACS 3.3 software package (29,30), using a simulation cell containing 75,170 water molecules. All atoms were treated in the OPLS-AA (optimized potentials for liquid simulations—all-atom) force field. The complete system was energy-minimized using a steepest descent algorithm. The MD simulation at 300 K (with 0.02 ps temperature bath coupling) was performed for 1 ns. During the simulation the integration time step was 1 fs, and the applied constant pressure was 1 bar. All simulations were performed on Pentium III processors running Linux.

RESULTS

$G\alpha_s$ bound structure of PTH1R(402-408)

The peptide is in fast exchange between the bound and the free state. The large negative NOEs observed in the trNOE spectrum verify that PTH1R(402–408) weakly binds $G\alpha_s$, as anticipated from our previous investigations (28). The seven amino acid C-terminus of IC3 adopts an α-helix structure while bound to $G\alpha_s$. The helix is amphipathic, with a well-defined hydrophilic face, expected to interact with solvent, and a hydrophobic face, expected to contact protein.

Saturation transfer difference spectroscopy

In the STD NMR experiment (31,32), $G\alpha_s$ is saturated with a selective saturation pulse. PTH1R(402–408), which is in exchange between the bound and the free form, becomes saturated when the peptide is bound to $G\alpha_s$. A difference spectrum is generated from subtracting the spectrum with protein saturation from the spectrum without protein saturation. The difference spectrum provides only the signals of the ligand residues most closely associated with the protein. The STD spectrum displays two peaks in the upfield aliphatic region at ~0.70 ppm and 0.76 ppm. These peaks were

assigned as the methyl groups of Leu-406 and Leu-407 in the trNOESY spectrum (Fig. 1). Two peaks in the aromatic region of the STD spectrum at 6.6 ppm and 6.8 ppm were assigned as the δ- and ϵ-carbons of Tyr-403 in the trNOESY spectrum (Fig. 1). The remaining peaks in the aliphatic region of the STD spectrum are located in overlapping β- and γ-carbon regions of the assigned trNOESY spectrum, so a definitive assignment of these peaks cannot be made. However, the peaks are likely to be the β-carbon of Leu-407, the β- or γ-carbon of Leu-406, and the γ-carbon of Lys-408 at 1.53 ppm, 1.40 ppm, and 1.26 ppm, respectively. The STD data supports the hypothesis that the hydrophobic face of PTH1R(402–408), composed of Tyr-403, Leu-406, and Leu-407, contacts Gα_s and that the hydrophilic face is exposed to solvent.

Model of PTH1R(402-408) in binding pocket of Gα_s

The crystal structure of Gα_s in complex with GTPγS (33) was used as a starting point for the molecular dynamics simulations. The crystal structure supports previous evidence from both alanine scanning and evolutionary trace analysis that the carboxy terminus, as well as the α4-β6 loop and the α5 helix, form the receptor contact site. The kink in the α5 helix places the carboxy terminus of the α5 helix in close contact to the α4-β6 loop. This positioning is stabilized by the side chain of M386 extending into the hydrophobic pocket created by the amino terminal residues of β5 and β6 (33). The surface created by the α5 helix and the α4-β6 loop is the predicted receptor contact site. The STD data orients the side chains of Tyr-403, Leu-406, and Leu-407 facing Gα_s. Simulations were performed on twenty initial conformations of the PTH1R(402–408) in complex with Gα_s to sample the tentative binding pocket. The most energetically stable complex was chosen for a longer molecular dynamics run. After 580 ps the hydrophilic side chains of Gln-402, Arg-404, Lys-405, Lys-408 residues remained solvent exposed and the hydrophobic Tyr-403, Leu-406, and Leu-407 residues were positioned in close proximity to Gα_s residues (Fig. 2). The model of PTH1R(402–408) and Gα_s after 580 ps of molecular dynamics is shown in Fig. 3. The hydroxyl of Tyr-403 is within hydrogen bonding distance from the hydroxyls of Y360 and S286, 2.6 Å and 2.8 Å, respectively. The δ- and ϵ-carbons of Tyr-403 are ~5 Å from Y358 with the two aromatic rings adopting a T-shaped orientation. Tyr-403 sits in the hydrophobic pocket of Gα_s ~4.5 Å above M386. The δC1 of Leu-406 is 3.8 Å from the side chain of R356, and the δC2 of Leu-406 is 4.5 Å from the backbone of R356. The δC1 of Leu-407 is 3.8 Å from the methyl of M386 and 3.6 Å and 4.0 Å from the β- and γ-carbons, respectively, of the side chain of Q390. The δC2 of Leu-407 is 3.6 Å from the β-carbon of T284. The β-carbon of Leu-407 is 4.8 Å from R389. Q390 contributes to the stabilization of the interaction between the α5 helix and the α4-β6 loop by extending into the hydrophobic pocket above M386.

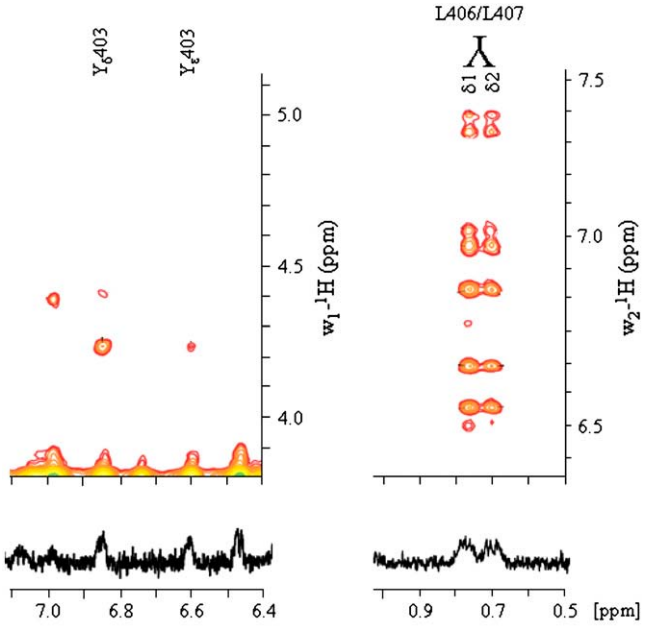

FIGURE 1 (*Top*) Expanded portion a TR-NOESY spectrum displaying NOEs of the δ- and ϵ-protons of Tyr-403 (*left*) and the NOEs of the methyl groups of Leu-406 and Leu-407 (*right*). (*Bottom*) Expanded portion of a difference STD spectrum, aligned with the assigned peaks from the TRNOESY. Resonances at 6.8, 6.6, 0.76, and 0.70 ppm correspond to the δ- and ϵ-protons of Y403 and the methyl groups of L406 and L407, respectively, which all contact Gα_s.

DISCUSSION

The C-terminal portion of the IC3 of the PTH1R has previously been identified as important for the signaling, and more

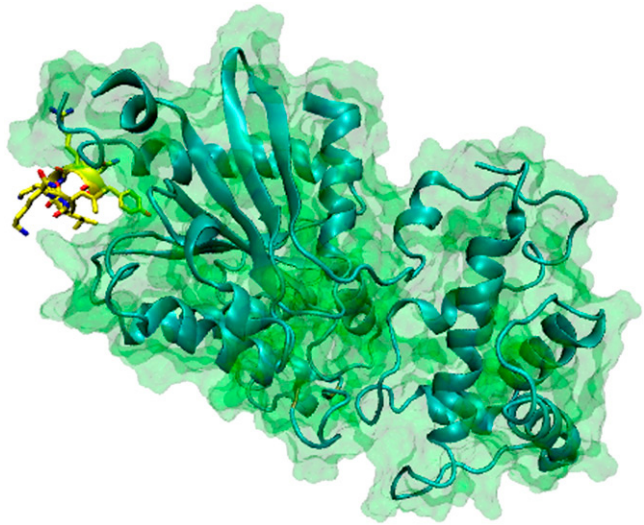

FIGURE 2 Interaction of PTH1R(402–408) (*yellow*) with Gα_s (*green ribbon*). The side chains of PTH1R are shown, with oxygens red and nitrogens blue.

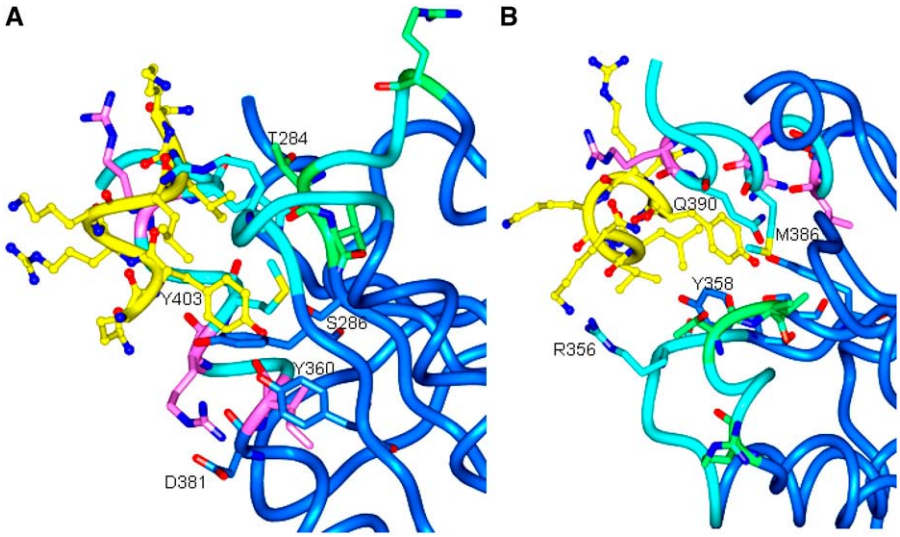

FIGURE 3 Two views (*B* is rotated 90°) of the interaction of PTH1R(402–408) interacting with $G\alpha_s$. The secondary structural elements of the $G\alpha_s$/receptor contact site, including the C-terminal residues of α5-helix (I382–L394), the α3-β5 loop and the α4-β6 loop, are colored in light blue. R389, R385, and I382, the residues that uncouple $G\alpha_s$ from GPCRs as a result of naturally occurring mutations, are highlighted in pink. R280, T284, and I285, the mutated residues in the α3-β5 loop that resulted in a decrease in receptor mediated accumulation of cAMP, are shown in green. The remaining residues of $G\alpha_s$ are dark blue, and PTH1R(402–408) is yellow.

importantly the G-protein specificity of the receptor. For the PTH receptor, Segre and co-workers have identified a number of important sites for $G\alpha_s$ activation (22), similar findings have been reported for a number of GPCRs using different mutagenic approaches, including insertion (21), and loss- (34–36) and gain-of-function (37–39). Here we have employed NMR methods to determine the structure and topological orientation of the C-terminus of IC3 of PTH1R while bound to $G\alpha_s$. The results indicate a well-defined amphiphilic α-helix with the hydrophobic face, including Tyr-403, Leu-406, and Leu-407, interacting with the protein.

The mode of interaction between the receptor and G-protein was refined by extensive, solvated MD simulations, providing a structural framework for the analysis of experimental and naturally occurring mutational data from previous studies. The ten most distal C-terminal amino acids of $G\alpha_s$ are crucial to forming the stable receptor binding site of $G\alpha_s$. M386 reaches into the hydrophobic pocket formed by the N-terminal residues of β5 and β6 (33). Q390 is also extended into this hydrophobic pocket (Fig. 3 *B*). These residues stabilize the interaction between the α5 helix and the α4-β6 loop. The uncoupling of receptors due to the $G\alpha_s$ genetic mutants ΔI382, R385H, and R389P can be explained by the model. I382 does not directly contact the peptide; however, deletion of this residue would disturb the essential orientation of the 10 most distal C-terminal residues in the α5 helix interacting with the α4-β6 loop and therefore disrupt the hydrophobic pocket of $G\alpha_s$. The bulky imidazole ring of histidine in the R385H mutant would block the binding pocket so that the tyrosine residue of PTH1R(402–408) is prevented from entering the pocket and forming important contacts with $G\alpha_s$. In addition, the positively charged guanidine group of the extended side chain of R385 is 2.7 Å from the negatively charged carboxy side chain of D381. The charge-charge interaction likely stabilizes the structure of the α5 helix. We can hypothesize that the R389P mutation causes a kink in the C-terminus away from the α4-β6 loop so that the orientation of the side chain of the key residue Q390 is altered. Furthermore, the β-carbon of Leu-407 is 4.8 Å from the β-carbon of R389. This hydrophobic contact contributes to the interaction between PTH1R(402–408) and $G\alpha_s$. Experimental mutational data suggest that the α3-β5 loop of $G\alpha_s$ is important for the receptor-mediated increase in production of cAMP. In the model, δC2 of Leu-407 is $<$4 Å from the β-methyl of T284, which is located in the α3-β5 loop. This hydrophobic interaction contributes to the removal of the highly hydrophobic leucine from solvent.

The PTH1R/$G\alpha_s$ model developed here is in accord with previous studies in addition to providing several previously unidentified residues making significant contributions in the receptor protein interaction. Tyr-403 is buried in the hydrophobic groove of $G\alpha_s$, forming hydrogen bonds with both Y360 and S286. Furthermore, Tyr-403 and Y358 are in a t-shaped position, providing additional stabilization of Tyr-403 by aromatic-aromatic interactions. R356, located in the α4-β6 loop, is in close proximity to Leu-406. The side chain of R356 extends outward so that the terminal amine groups contact solvent, and the remainder of the side chain shields δC1 of Leu-406 from solvent. Furthermore, the backbone of R356 is 4.5 Å from δC2 of Leu-406. The model predicts that mutating residues Y360, S286, Y358, and R356 will disturb the association of $G\alpha_s$ to PTH1R and thus lead to a reduction of receptor-mediated accumulation of cAMP.

PTH1R(402–408) inserts the hydrophobic residues Tyr-403, Leu-406, and Leu-407 in to a hydrophobic groove formed by several secondary structural elements of $G\alpha_s$ (Fig. 4). The hydrophobic pocket is mainly formed from the C-terminal α5 helix, the α4-β6 loop and β6. In addition, residues T284 and S286 from the α3-β5 loop and β5, respectively, contribute to the back of the pocket. The transient and reversible interaction between $G\alpha_s$ and PTH1R is largely driven by the nonpolar groups of the receptor

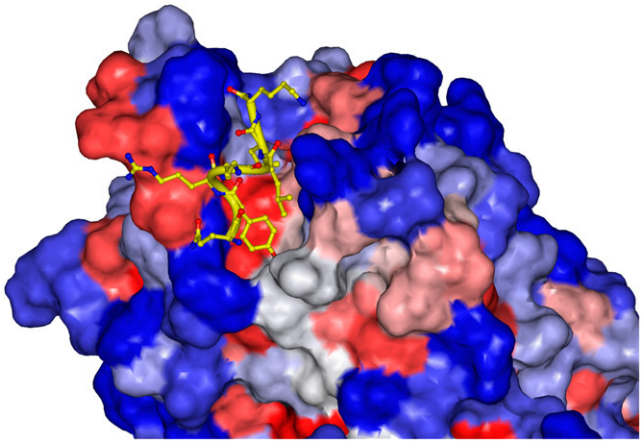

FIGURE 4 Top view of PTH1R(402–408) (*yellow*, with oxygens and nitrogens, *red* and *blue*) bound within the hydrophobic groove of $G\alpha_s$ (colored by hydrophobicity, with *red* hydrophobic, *blue* charged).

interacting with the hydrophobic groove of $G\alpha_s$. Strong charge-charge interactions between $G\alpha_s$ and PTH1R that would lead to a tight association are avoided, consistent with the general model of G-protein activation and signaling pathways.

Incorporating the IC3 domain into the entire seven-transmembrane, PTH receptor provides the overall topology of the interaction of $G\alpha_s$ with PTH1R. The portion of PTH1R that contacts $G\alpha_s$ is adjacent to transmembrane helix six and continues the α-helical structure of TM6. Just N-terminal of this region, there is a flexible portion of the IC3 loop, as previously determined by high-resolution NMR (23). The superposition of PTH1R(402–408) onto the corresponding residues of the full structure of PTH1R does not lead to any steric clashes or overlap with the x-ray structure of $G\alpha_s$. In Fig. 5, the solvent exposed groove of $G\alpha_s$ fits tightly against the helix-loop-helix surface of IC3. Additionally, the hydrophobic residues of PTH1R(402–408) face the hydrophobic pocket of $G\alpha_s$. The model proposed here, of the interaction of PTH1R with $G\alpha_s$ provides for insight into the intricate, highly specific signaling profile of PTH1R. Future studies will utilize the proposed structural framework to aid in the elucidation of the specificity of PTH1R coupling to $G\alpha_s$ and $G\alpha_q$.

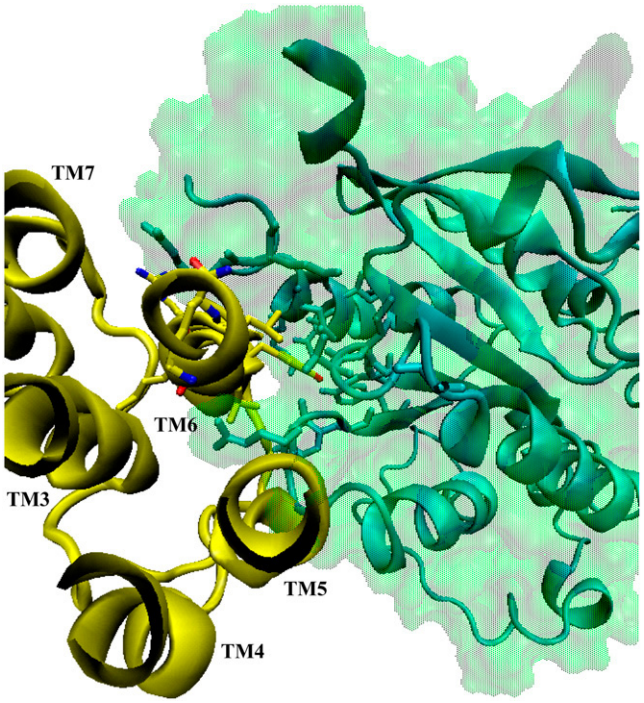

FIGURE 5 Association, from the extracellular surface, of $G\alpha_s$ (*green*) with PTH1R (*yellow*). The side chains of PTH1R(402–408) and many residues of $G\alpha_s$, described in the text and detailed in Fig. 3, are illustrated for reference.

The authors thank Dr. Maria Pellegrini, Biogen-Idec, for assistance with the NMR experiments.

The research was supported, in part, by the National Institutes of Health through GM-54082.

REFERENCES

1. Dempster, D. W., F. Cosman, M. Parisien, V. Shen, and R. Lindsay. 1993. Anabolic actions of parathyroid hormone on bone. *Endocr. Rev.* 14:690–709.
2. Chorev, M., and M. Rosenblatt. 1994. Structure function analysis of parathyroid hormone and parathyroid hormone-related protein. *In* The Parathyroids. J.P. Bilezikian, M. A. Levine, and R. Marcus, editors. Raven Press, New York. 139–156.
3. Abou-Samra, A.-B., H. Jüppner, T. Force, M. W. Freeman, X. F. Kong, E. Schipani, P. Urena, J. Richards, J. V. Bonventre, J. T. Potts, Jr., H. Kronenberg, and G. V. Segre. 1992. Expression cloning of a common receptor for parathyroid hormone and parathyroid hormone-related peptide from rat osteoblast-like cells: a single receptor stimulates intracellular accumulation of both cAMP and inositol trisphosphates and increases intracellular free calcium. *Proc. Natl. Acad. Sci. USA.* 89:2732–2736.
4. Civitelli, R., T. J. Martin, A. Fausto, S. L. Gunsten, K. A. Hruska, and L. V. Avioli. 1989. Parathyroid hormone-related peptide transiently increases cytosolic calcium in osteoblast-like cells: comparison with parathyroid hormone. *Endocrinology.* 125:1204–1210.
5. Pines, M., S. Fukuyama, K. Costas, E. M. Meurer, P. K. Goldsmith, X. Xu, S. Muallem, V. Behar, M. Chorev, M. Rosenblatt, A. H. Tashjian, Jr., and L. J. Suva. 1996. Inositol 1-,4-,5-trisphosphate-dependent Ca^{2+} signaling by the recombinant human PTH/PTHrP receptor stably expressed in a human kidney cell line. *Bone.* 18:381–389.
6. Hedin, K. E., K. Duerson, and D. E. Clapham. 1993. Specificity of receptor-G protein interactions: Searching for the structure behind the signal. *Cell. Signal.* 5:505–518.
7. Savarese, T. M., and C. M. Fraser. 1992. In vitro mutagenesis and the search for structure-function relationships among G protein-coupled receptors. *Biochem. J.* 283:1–19.
8. Conklin, B. R., and H. R. Bourne. 1993. Structural elements of $G\alpha$ subunits that interact with $G\beta\gamma$, receptors, and effectors. *Cell.* 73: 631–641.
9. Spiegel, A. M., W. F. Simonds, T. L. Jones, P. K. Goldsmith, and C. G. Unson. 1990. *Biochem. Soc. Symp.* 56:61–69.
10. Simonds, W. F., P. K. Goldsmith, C. J. Woodard, C. G. Unson, and A. M. Spiegel. 1989. Receptor and effector interactions of G_s functional studies with antibodies to the α_s carboxyl-terminal decapeptide. *FEBS Lett.* 249:189–194.

11. Pantaloni, C., and Y. Audigier. 1993. Functional domains of the Gs alpha subunit: role of the C-terminus in the receptor-dependent and receptor-independent activation. *J. Recept. Res.* 13:591–608.

12. Schwindinger, W. F. 1994. A novel $G_s\alpha$ mutant in a patient with Albright hereditary osteodystrophy uncouples cell surface receptors from adenylyl cyclase. *J. Biol. Chem.* 269:25387–25391.

13. Sullivan, K. A., R. T. Miller, S. B. Masters, B. Beiderman, W. Heideman, and H. R. Bourne. 1987. Identification of receptor contact site involved in receptor−G protein coupling. *Nature.* 330:758–760.

14. Rall, T., and B. A. Harris. 1987. Identification of the lesion in the stimulatory GTP-binding protein of the uncoupled S49 lymphoma. *FEBS Lett.* 224:365–371.

15. Reference deleted in proof.

16. Wu, W. I., W. F. Schwindinger, L. F. Aparicio, and M. A. Levine. 2001. Selective resistance to parathyroid hormone caused by a novel uncoupling mutation in the carboxyl terminus of $G\alpha_s$. A cause of Pseudohypoparathyroidism type Ib. *J. Biol. Chem.* 276:165–171.

17. Conklin, B. R., S. Ishida, T. Voyno-Yasenetskaya, Y. Sun, Z. Farfel, and H. R. Bourne. 1996. Carboxyl-terminal mutations of $G_q\alpha$ and $G_s\alpha$ that alter the fidelity of receptor activation. *Mol. Pharmacol.* 50:885–890.

18. Lee, C. H., A. Katz, and M. I. Simon. 1995. Multiple regions of $G_{\alpha 16}$ contribute to the specificity of activation by the C5a receptor. *Mol. Pharmacol.* 47:218–223.

19. Grishina, G., and C. Berlot. 2000. A surface-exposed region of $G_{s\alpha}$ in which substitutions decrease receptor-mediated activation and increase receptor affinity. *Mol. Pharmacol.* 57:1081–1092.

20. Lichtarge, O., H. R. Bourne, and F. Cohen. 1996. Evolutionarily conserved $G_\alpha\beta\gamma$ binding surfaces support a model of the G-protein-receptor complex. *Proc. Natl. Acad. Sci. USA.* 93:7507–7511.

21. Strader, C. D., T. M. Fong, M. R. Tota, D. Underwood, and R. A. F. Dixon. 1994. Structure and function of G protein-coupled receptors. *Annu. Rev. Biochem.* 63:101–132.

22. Komatsu, Y., and G. V. Segre. 1998. Interactions between the intracellular domains of the PTH/PTHrP receptor and trimeric G proteins. *In* American Society for Bone and Mineral Research. Elsevier, San Francisco. S253.

23. Pellegrini, M., M. Royo, M. Chorev, and D. F. Mierke. 1996. Conformational characterization of a peptide mimetic of the third cytoplasmic loop of the G-protein coupled parathyroid hormone/parathyroid hormone related protein receptor. *Biopolymers.* 40:653–666.

24. Mierke, D. F., M. Royo, M. Pellegrini, H. Sun, and M. Chorev. 1996. Peptide mimetic of the third cytoplasmic loop of the PTH/PTHrP receptor. *J. Am. Chem. Soc.* 118:8998–9004.

25. Mayer, M., and B. Meyer. 2000. Mapping the active site of angiotensin-converting enzyme by transferred NOE spectroscopy. *J. Med. Chem.* 43:2093–2099.

26. Haselhorst, T., J. F. Espinosa, J. Jimenez-Barbero, T. Sokolowski, P. Kosma, H. Brade, L. Brade, and T. Peters. 1999. NMR experiments reveal distinct antibody-bound conformations of a synthetic disaccharide representing a general structural element of bacterial lipopolysaccharide epitopes. *Biochemistry.* 38:6449–6459.

27. Meyer, B., T. Weimar, and T. Peters. 1997. Screening mixtures for biological activity by NMR. *Eur. J. Biomchem.* 246:705–709.

28. Ulfers, A. L., J. L. McMurry, A. Miller, L. Wang, D. A. Kendall, and D. F. Mierke. 2002. Cannabinoid receptor-G protein interactions: $G_{\alpha i1}$-bound structures of IC3 and a mutant with altered G-protein specificity. *Protien Sci.* 11:2526–2531.

29. Lindahl, E., B. Hess, and D. van der Spoel. 2001. GROMACS 3.0: a package for molecular simulation and trajectory analysis. *J. Mol. Mod.* 7:306–317.

30. Berendsen, H. J. C., D. van der Spoel, and R. van Drunen. 1995. GROMACS: a message-passing parallel molecular dynamics implementation. *Comp. Phys. Comm.* 91:43–56.

31. Mayer, M., and B. Meyer. 1999. Characterization of ligand binding by saturation transfer difference NMR spectroscopy. *Angew. Chem. Int. Ed. Engl.* 38:1784–1788.

32. Mayer, M., and B. Meyer. 2001. Group epitope mapping by saturation transfer difference NMR to identify segments of a ligand in direct contact with a protein receptor. *J. Am. Chem. Soc.* 123:6108–6117.

33. Sunahara, R. K., J. J. Tesmer, A. G. Gilman, and S. R. Sprang. 1997. Crystal structure of the adenylyl cyclase activator $G_{s\alpha}$. *Science.* 278: 1943–1947.

34. Liu, J., N. Blin, B. R. Conklin, and J. Wess. 1996. Molecular mechanisms involved in muscarinic acetylcholine receptor-mediated G-protein activation studied by insertion mutagenesis. *J. Biol. Chem.* 271:6172–6178.

35. Kosugi, S., F. Okajima, T. Ban, A. Hidaka, A. Shenker, and L. D. Kohn. 1992. Mutation of alanine 623 in the third cytoplasmic loop of the rat thyrotropin (TSH) receptor results in a loss in the phosphoinositide but not cAMP signal induced by TSH and receptor autoantibodies. *J. Biol. Chem.* 267:24153–24156.

36. Cotecchia, S., S. Exum, M. G. Caron, and R. J. Lefkowitz. 1990. Regions of the 1-adrenergic receptor involved in coupling to phosphatidylinositol hydrolysis and enhanced sensitivity of biological function. *Proc. Natl. Acad. Sci. USA.* 87:2896–2900.

37. Högger, P., M. S. Shockley, J. Lameh, and W. Sadee. 1995. Activating and inactivating mutations in N- and C-terminal i3 loop junctions of muscarinic acetylcholine Hm1 receptors. *J. Biol. Chem.* 270: 7405–7410.

38. Liggett, S. B., M. G. Caron, R. J. Lefkowitz, and M. Hnatowich. 1991. Coupling of a mutated form of the human β2-adrenergic receptor to G_i and G_s. Requirement for multiple cytoplasmic domains in the coupling process. *J. Biol. Chem.* 266:4816–4821.

39. Blin, N., J. Yun, and J. Wess. 1995. Mapping of single amino acid residues required for selective activation of $G_{q/11}$ by the m3 muscarinic acetylcholine receptor. *J. Biol. Chem.* 270:17741–17748.